

Article

Historical and Projected Trends of the Mean Surface Temperature in South-Southeast Mexico Using ERA5 and CMIP6

Mercedes Andrade-Velázquez^{1,*} and Martín José Montero-Martínez^{2,*} 

¹ Cátedra CONACYT—Centro del Cambio Global y la Sustentabilidad (CCGS), Calle Centenario del Instituto Juárez S/N, Colonia Reforma, Villahermosa CP 86080, Mexico

² Instituto Mexicano de Tecnología del Agua, Subcoordinación de Eventos Extremos y Cambio Climático, Paseo Cuauhnáhuac 8532, Colonia Progreso, Jiutepec CP 62550, Mexico

* Correspondence: mercedes.andrade@ccgs.mx (M.A.-V.); martin_montero@tlaloc.imta.mx (M.J.M.-M.)

Abstract: This study aimed to determine the mean temperature trends in the south-southeast region of Mexico during the historical period of 1980–2014, as well as during the future periods of 2021–2040, 2041–2060, and 2081–2100, as recommended by the IPCC. Additionally, the study sought to identify the climate change scenario that is most closely aligned with the socio-environmental conditions of the south-southeast zone of Mexico and that has the greatest impact on the region's average temperature. The downscaling method of bias correction was conducted at a spatial resolution of $0.25^\circ \times 0.25^\circ$, and an analysis of historical trends was performed for the period 1980–2014 with ERA5 and four CMIP6 models (CNRM-ESM2-1, IPSL-CM6A-LR, MIROC6, and MRI-ESM2-0). This process was extended to future projections. The models indicated temperature differences of less than 0.5°C with respect to ERA5, in agreement with other studies. Additionally, the current study calculated future trends for the south-southeast region using three of the CMIP6 scenarios (SSP2-4.5, SSP4-6.0, and SSP5-8.5). The *z- ϵ* proposal was used to compare the slopes, enabling us to determine which of the three scenarios corresponded to the historical trend, assuming identical socio-environmental conditions. The SSP4-6.0 scenario was found to correspond to the historical trend.

Keywords: climate change; south-southeast Mexico; CMIP6; temperature trend; bias correction



Citation: Andrade-Velázquez, M.; Montero-Martínez, M.J. Historical and Projected Trends of the Mean Surface Temperature in South-Southeast Mexico Using ERA5 and CMIP6. *Climate* **2023**, *11*, 111. <https://doi.org/10.3390/cli11050111>

Academic Editors: Nir Y. Krakauer and Konstantia Tolika

Received: 15 March 2023

Revised: 12 May 2023

Accepted: 16 May 2023

Published: 18 May 2023



Copyright: © 2023 by the authors. Licensee MDPI, Basel, Switzerland. This article is an open access article distributed under the terms and conditions of the Creative Commons Attribution (CC BY) license (<https://creativecommons.org/licenses/by/4.0/>).

1. Introduction

Currently, the impacts of climate change in the world are alarming. The Third Assessment Report (TAR) of the Intergovernmental Panel on Climate Change (IPCC) has reported that meteorological events will increase in intensity and frequency due to global warming [1,2]. This finding has been confirmed in subsequent reports, including the IPCC-AR5, which indicated that the changes in the world's climate are due to the influence of climate modulators such as ENSO, transferring their effects to different regions [3].

Updating and improving the climatic information allows for the development of better strategies for adaptation to climate change. This is exemplified by the scenarios developed within the framework of the Coupled Model Intercomparison Project Phase 6 (CMIP6) [4]. CMIP6 uses a matrix model that combines physical processes of the climate (Representative Concentration Pathways, RCP) with human actions or measures (shared socioeconomic pathways, SSP), resulting in eight large groups of scenarios: SSP1-1.9, SSP1-2.6, SSP2-4.5, SSP3-7.0, SSP4-3.4, SSP4-6.0, SSP5-3.4-OS, and SSP5-8.5 [4]. Further details can be found in [4]. These scenarios provide valuable insights for understanding and addressing the impacts of climate change.

These scenarios concern the possible future evolution due to anthropogenic forcings from greenhouse gas (GHG) emissions, based on the RCPs. High and very high emissions refer to SSP3-7.0 and SSP5-8.5, where each doubles the CO₂ emissions in 2100 and 2050,

respectively. In the case of intermediate emissions, that is, at current levels up to mid-century, the scenarios are SSP2-4.5 and SSP4-6.0, while low and very low GHG emissions, which decrease in 2050, correspond to SSP1-1.9 and SSP1-2.6 [5]. The SSP families that constitute these scenarios are defined as follows [6]:

- SSP1: Sustainable and equitable, where the common good is preserved and nature is respected, social inequalities are reduced, and consumption is oriented towards minimizing the use of energy and material resources.
- SSP2: The middle of the road, which extrapolates current and past developments into the future. The environmental system is degraded. Population growth is moderate. Cooperation between nations is limited, and there are significant differences in countries' incomes.
- SSP3: Regional rivalry. National and regional conflicts. Investments in technological and educational development are decreasing. Inequality increases, and some regions suffer drastic environmental damage.
- SSP4: Inequality pathway. There is a gap between societies, and their cooperation, income, and education are low. Environmental problems are only resolved locally in some regions but not in others.
- SSP5: Fossil-fuel-based development pathway. The global market is integrated, and there is technological progress. However, social and economic development is based on the exploitation of oil. There is a high demand for energy.

Most of the CMIP6 models seem to capture the main features of spatial variations in the observed global temperature (typical correlation pattern ≥ 0.98), but with large variability among models and regions [7]. The CMIP6 models have a wider range of climate sensitivity than the CMIP5, which may be due to the cloud amplifier of the CMIP6 corresponding to 20% [7]. In addition, the mean of CMIP6 can capture the observed global surface temperature trends during 1901–1940 (warming), 1941–1970 (cooling), and 1971–2014 (rapid warming) [7]. To date, several studies have been conducted at the regional level on the changes found in the projections of various climatic variables of CMIP6 compared with previous phases, such as CMIP5. Examples include Africa [8], Australia [9], and China [10].

In Mexico, different authors have worked with information from CMIP3 and CMIP5 [11–13]. The REA method [14] was used by [12] to generate climate scenarios, which provided a new update to the management of CMIP5 data. Within the CMIP5, the RCP8.5 scenario is considered the most extreme scenario in terms of the maximum radiative forcing that could be reached at the end of this century. However, there are two other scenarios of lesser magnitude, such as RCP4.5 and RCP6.0. According to [15], RCP6.0 is the “appropriate” scenario for southeastern Mexico, Central America, and the Caribbean, since this region has experienced a similar warming rate historically.

However, a similar process remains to be conducted with the CMIP6 scenarios. For this, downscaling techniques must be used, either dynamic or statistical [16–18], each with its advantages and disadvantages [19]. Among the statistical techniques, the categories of analogs, time generators, and regressions stand out [20]. The IPCC, in its sixth assessment report (AR6), showed that the perfect prognosis method had greater confidence than the analog method and stochastic regression [21]. Additionally, bias correction is a technique used to remove bias and uncertainty from global models [16], and it indicates greater confidence in the improvement in the distribution of the simulated variables. The bias correction technique scales the output of the climate model and systematizes its errors, improving the fit to the observations [17].

To examine if the new scenario information generated by CMIP6 continued the same pattern of trends observed for CMIP5, the present study analyzed the trends in temperature in the historical period and determined if the rate of warming was in correspondence with the SSP4-6.0 scenario for the southeastern and southern region of Mexico. The method, results, discussion, and conclusions are described below.

2. Materials and Methods

2.1. Study Zone

The south-southeast zone of Mexico is relevant because of its biocultural richness and natural resources [22]. It is currently a strategic area of economic development, given the investment in infrastructure in recent years [23]. In addition, in this area, there is a large migratory flow of individuals from Central America, the Caribbean, and Latin America [24]. It is an area exposed to different meteorologic and climatic phenomena (Figure 1), such as tropical cyclones and cold fronts, as well as the impacts of the influence of El Niño-Southern Oscillation (ENSO) [25]. A warming trend of approximately 10^{-2} °C/year was shown by [15] for this area, which is in correspondence with the rate of warming under the RCP 6.0 scenario. For precipitation, a trend is not noticeable. However, [26] indicated important changes in the precipitation patterns, such as wet events that have occurred mainly in the Grijalva-Usumacinta basin (GUB) in recent years. The GUB is located in the study region, which is of great environmental and social importance for Mexico and Central America [27]. It is a system that can allow ecosystem-based adaptation to climate change [27].

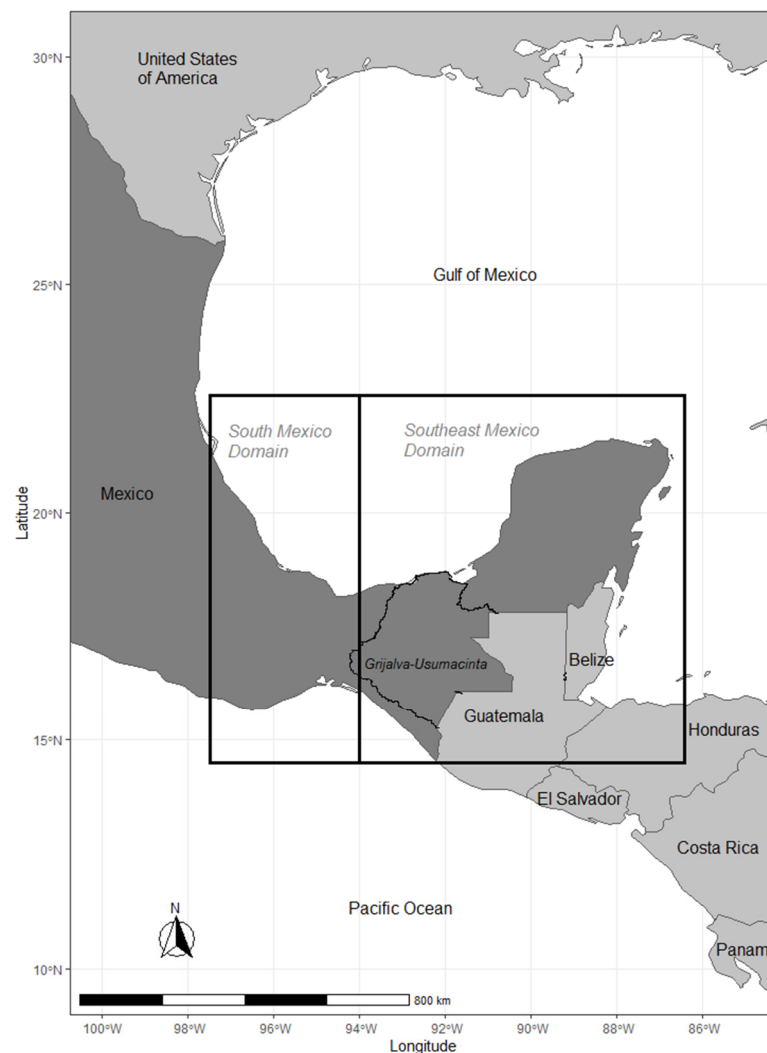


Figure 1. Study area, showing the southern and southeastern domains of Mexico.

2.2. Methods

The mean near-surface air temperature (tas) data used here correspond to the ERA5 database [28] of historical data. The global climate models (GCMs) listed in Table 1 were selected according to the analysis of [29]. They showed that CMIP6 models [4] had better

performance regarding the local historical climate of the study area. We noted that two of the selected models performed well for regions such as Guatemala [30]. The resolution of the data is shown in Table 1. A mask was applied for the mainland region and regridded to 25 km × 25 km to obtain the information on a smaller scale (the original scale is shown in Table 1). The selected periods were based on what was suggested by [21].

Table 1. Data used for the mean surface temperature (tas) from ERA5 [28] and the three CMIP6 scenarios with four models [31–46]. License: CC by 4.0 (<https://creativecommons.org/licenses/by/4.0/>, accessed on 15 March 2023).

Number	Data	Resolution	Variable	Time	Scenario
1	ERA5	25 km × 25 km	tas	1980–2014	
2	CNRM-ESM2-1	250 km × 250 km	tas	1980–2014 2021–2040 2041–2060 2081–2100	SSP2-4.5, SSP4-6.0, SSP5-8.5
3	IPSL-CM6A-LR	250 km × 250 km	tas	1980–2014 2021–2040 2041–2060 2081–2100	SSP2-4.5, SSP4-6.0, SSP5-8.5
4	MIROC6	250 km × 250 km	tas	1980–2014 2021–2040 2041–2060 2081–2100	SSP2-4.5, SSP4-6.0, SSP5-8.5
5	MRI-ESM2-0	100 km × 100 km	tas	1980–2014 2021–2040 2041–2060 2081–2100	SSP2-4.5, SSP4-6.0, SSP5-8.5

With the GCMs, the statistical scale reduction technique known as bias correction (see Equation (1)) [17] was applied, which allowed us to optimize the global information of the models at a local scale. This method is suggested for the temperature variable and is suitable for daily data

$$T_{corr,i} = T_{mod,i} + dT_i$$

where

$$dT_i = T_{ERA5,i} - T_{mod,i}$$
(1)

Here, the subscript *mod* refers to the model data, the subscript *i* refers to each day throughout the record, and dT_i is the difference between the historical means of the model and ERA5. For the current case, the equation indicates the bias obtained from the historical period 1980–2014 regarding the ERA5 for the same period. To determine the confidence of the technique, we applied the root mean square deviation (also known as the root mean square error, rmse) (rmsd) for the historical data of the models regarding the mean of the ERA5 data.

2.3. Temperature Trends

To calculate the trends, first, the information was considered only for Mexico in the south-southeast region (see Figure 1). Then the south-southeast region was divided into two: the south, which included the states of Veracruz, Oaxaca and Puebla; and the southeast, which included the states of Chiapas, Tabasco, Quintana Roo, Campeche, and Yucatán [47]. This was carried out to consider the domains in Mexico of the CORDEX Flagship Pilot Study project “North America: Dynamical downscaling experiments and hydrological modelling for Canada and Mexico” (<https://cordex.org/experiment-guidelines/flagship-pilot-studies/endorsed-cordex-flagship-pilote-studies/north-america-dynamical-downscaling-experiments-and-hydrological-modelling-for-canada-and-mexico/>, accessed on 15 March 2023) in the southern region. The southeastern part of Mexico allowed us to compare the

results with [15]. The areal average for each region was taken, and the trend was calculated on the basis of historical data and projections under the three scenarios (SSP2-4.5, SSP4-6.0, and SSP5-8.5). The Mann-Kendall test was used to adjust the trend [48,49].

In addition, we also used the *z-eq* value [50,51] defined by

$$z = \frac{m_1 - m_2}{(SE_{m_1} + SE_{m_2})^{1/2}}$$

where m_1 corresponds to the slope in the ERA5 data and m_2 corresponds to the slope of each model (Table 1), and SE_{m_1} and SE_{m_2} correspond to the standard errors associated with m_1 and m_2 respectively. The statistical significance of z is between the values of -1.96 and 1.96 . In this case, we can say that the slopes are similar, in addition to the case of $z = 0$. The value of *z-eq* allowed us to compare the slopes and find their differences or similarities weighted by the square root of the associated errors. In the case of $z = 0$, it was found that m_1 and m_2 were equal. In the case of $-1.96 < z < 1.96$, there were differences between m_1 and m_2 that fell within the range of their associated errors. This then guided whether the trend found could be maintained or changed drastically in the periods of time under study. For more details, see [15].

The climate change scenarios display a very similar evolution of radiative forcing in the near future. This indicates that the rate of the increase in temperature is also similar among the scenarios. It is difficult to differentiate them during the approximately 35-year period from 2000 to 2035 [52]. Therefore, we proposed extrapolating the historical rate of increase to that period, assuming that the socio-environmental conditions have remained the same. This approach helped us identify the most similar climate change scenario.

3. Results

3.1. Bias Correction

For the case of bias correction, Figure 2a shows the daily climatology of the ERA5 data and the models (Table 1) without correction, and Figure 2b indicates the same data after applying the bias correction to the models. The rmsd associated with the data from the models without bias correction regarding the observations (ERA5) was 1.444 °C for CNRM-ESM2-1, 1.498 °C for IPSL-CM6A-LR, 3.050 °C for MIROC6, and 1.411 °C for MRI-ESM2-0, while the error associated with the models with bias correction regarding the observations was 0.325 °C for CNRM-ESM2-1, 0.361 °C for IPSL-CM6A-LR, 0.493 °C for MIROC6, and 0.342 °C for MRI-ESM2-0. We noted that the bias correction optimized the records. These results are similar to those of [53], who reported a bias of 0.2 °C for a broader area towards Central America using an ensemble of models and a comparison with the CRU database [54]. Additionally, the authors reported that the discrepancy in the bias could be attributed to the reference database.

The historical bias results for each model in the historical period are shown in Figure S1. We can see that the bias correction optimized the model data by recording the climate patterns of the area recorded in ERA5. We applied the direct correction to the data of the projections of the three climate change scenarios for the three future periods (see Table 1).

3.2. Data Trends

In the data corrected for bias, annual trends were obtained for each region (south and southeast; see Figure 1) of the study area, where the majority showed a good fit (see Table S1). Note that the slope of the model data was bias-corrected. All the trends were positive, indicating warming with the same order of magnitude (10^{-2} °C/year). This was also observed in the historical trends both in ERA5 and in the models (see Table S2). From what we could observe, as indicated by [16] for the southeast region, both regions had the same warming rate. This has also been reported by other authors, such as [55,56], with an order of magnitude of 10^{-2} °C/year. On the other hand, [57] reported an increase of 0.7 °C in Mexico over the span of seven decades from 1951 to 2017, which equates to an increase of 0.1 °C per decade. The same author also reported an increase of 0.2 °C per decade in

the south-southeast region of Mexico. These findings aligned with the trend calculated by other authors, thereby validating the results of this study.

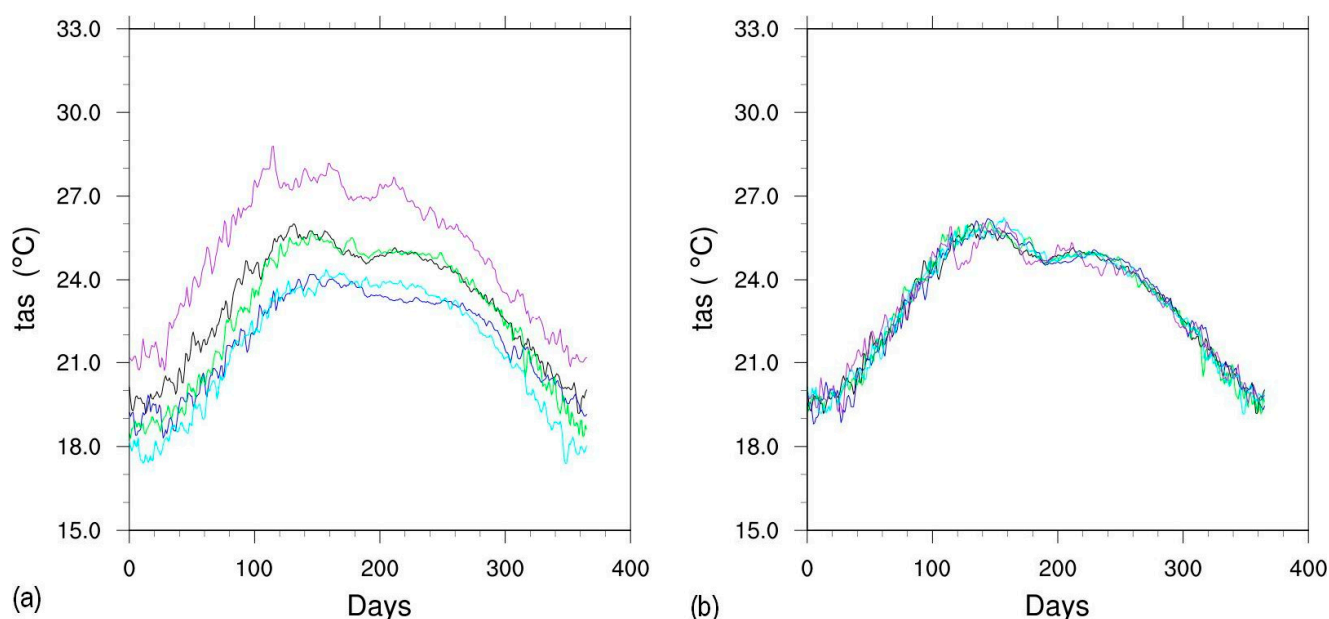


Figure 2. (a) Daily climatology of the mean surface temperature ($^{\circ}\text{C}$) without bias correction applied to the models for the south-southeast region of Mexico (ERA5 is shown in black, the CNRM-ESM2 model is in cyan, the IPSL-CM6A-LR model is in blue, the MIROC6 model is in purple, and the MRI-ESM2-0 model is in green). (b) The same as in (a) but with bias correction applied to the models.

We determined an ERA trend of $0.01\text{ }^{\circ}\text{C}$ per year for the southern region and $0.04\text{ }^{\circ}\text{C}$ per year for the southeast region. The average trend for both regions was $0.025\text{ }^{\circ}\text{C}$ per year. On the other hand, [56] determined a trend of $0.023\text{ }^{\circ}\text{C}$ per year for both regions. Our results provided trends for each region, taking their climatic differences into account. The southern region is less humid than the southeast, with average temperatures of $21\text{ }^{\circ}\text{C}$ and $26\text{ }^{\circ}\text{C}$, respectively [58]. This study determined the trends for both regions. Although the warming in the southern region was of the same order as that in the southeast region, the rate of warming was lower in the latter. We suggest that this may be due to a greater altitude gradient in the southern zone as compared with the southeast, owing to the presence of mountain ranges in the former. Additionally, the southern region covers a broader extension towards more northerly latitudes. This is why we divided the study area into two regions.

In the case of the models, the trends were positive in both regions. Each model indicated the same trend for both regions, which suggests that they underestimated the rate of warming for the southeastern region ($\leq 0.02\text{ }^{\circ}\text{C}/\text{year}$) and overestimated it for the southern region ($\geq 0.02\text{ }^{\circ}\text{C}/\text{year}$). We assume that this is because the models may encompass the entire region with the same orographic or climatic conditions, resulting in an equal warming trend for both regions. It should be noted that if both regions are taken into consideration, the difference with respect to the average trend would be less than or equal to $0.01\text{ }^{\circ}\text{C}/\text{year}$. This is consistent with the rmsd obtained by applying bias correction.

The trends for the periods 2021–2040, 2041–2060, and 2081–2100 were also determined for each of the models and scenarios (SSP2-4.5, SSP4-6.0, and SSP5.8.5).

The evolution of the radiative forcing for SSP2-4.5 increased until 2080 and stabilized by the end of the century, reaching $4.5\text{ W}/\text{m}^2$. For SSP4-6.0, it increased until the end of the century (and reached $6.0\text{ W}/\text{m}^2$), with a greater slope than for SSP2-4.5. For SSP5-8.5, it increased until the end of the century, with a much greater slope than the other two [52]. This evolution is in correspondence with the projected change in the global average temperature. Similarly, in the southeast region, the results of the mean temperature

trends for the SSP2-4.5 scenario were lower than those for SSP4-6.0 and much lower than those for SSP5-8.5. The results for both regions agreed with those of [53]. However, we noted that the SSP2-4.5 and SSP4-6.0 scenarios for the period 2081–2100 indicated a lower trend, a sign of their stability for that period (Figures 3 and 4).

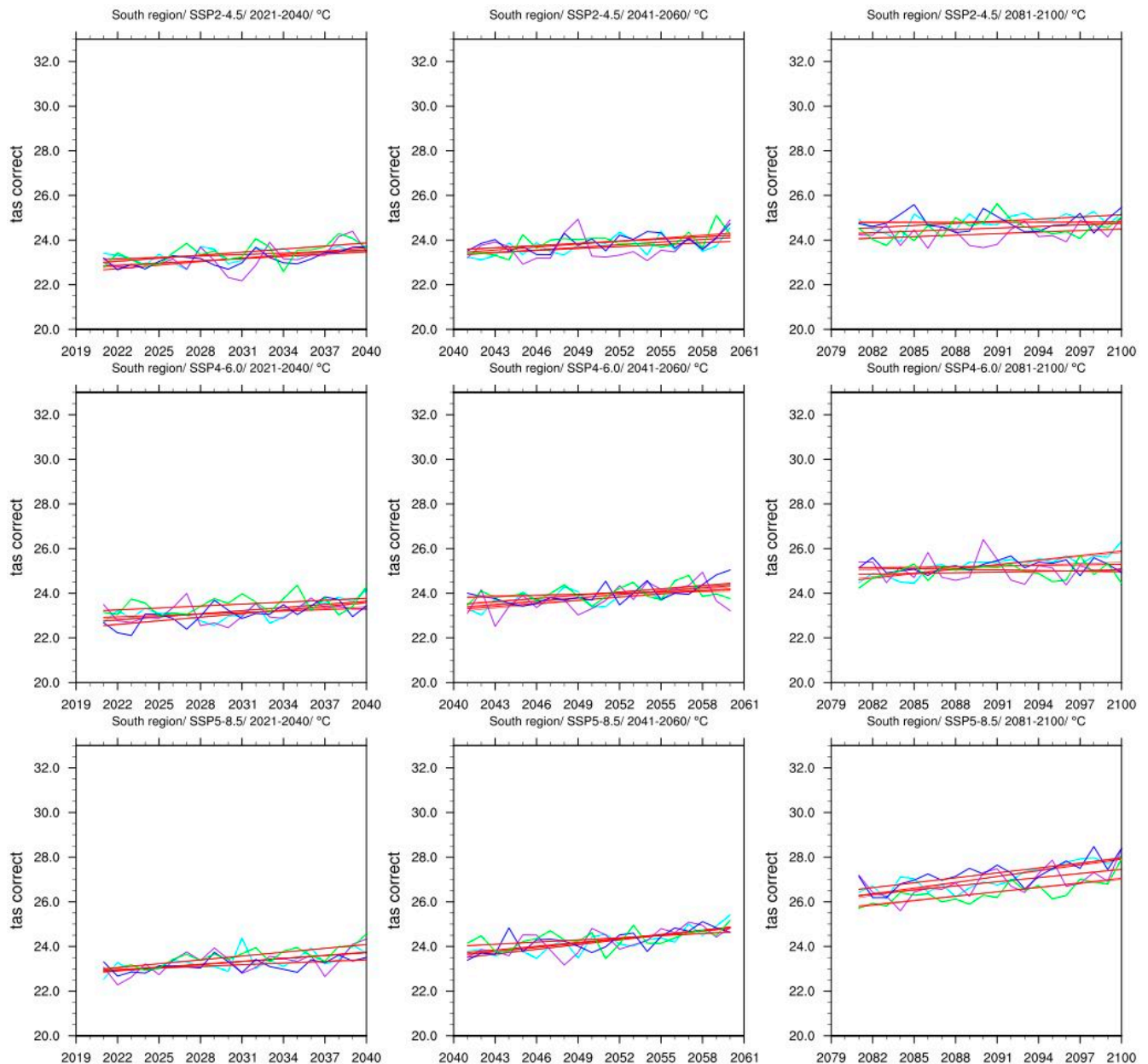


Figure 3. Annual projections of the average surface temperature (tas) for the southern region, under three scenarios SSP2-4.5 (first row), SSP4-6.0 (second row), and SSP5-8.5 (third row) for the different future periods, namely 2021–2040 (first column), 2041–2060 (second column), and 2081–2100 (third column), with the four models CNRM-ESM2-1 (cyan), IPSL-CM6A-LR (blue), MIROC6 (purple), and MRI-ESM2-0 (green).

It is worth noting that determining the likelihood of any one scenario occurring during the current period is a challenging task, given that warming rates can vary depending on the socio-environmental conditions affecting the region and the planet. Therefore, each scenario has an equal probability of occurring. For the near future (2021–2040), all three scenarios exhibited a similar range of temperature variability in both regions. The

same was true for the medium term (2041–2060). However, the differences between the three scenarios become more apparent in the long term (2081–2100).

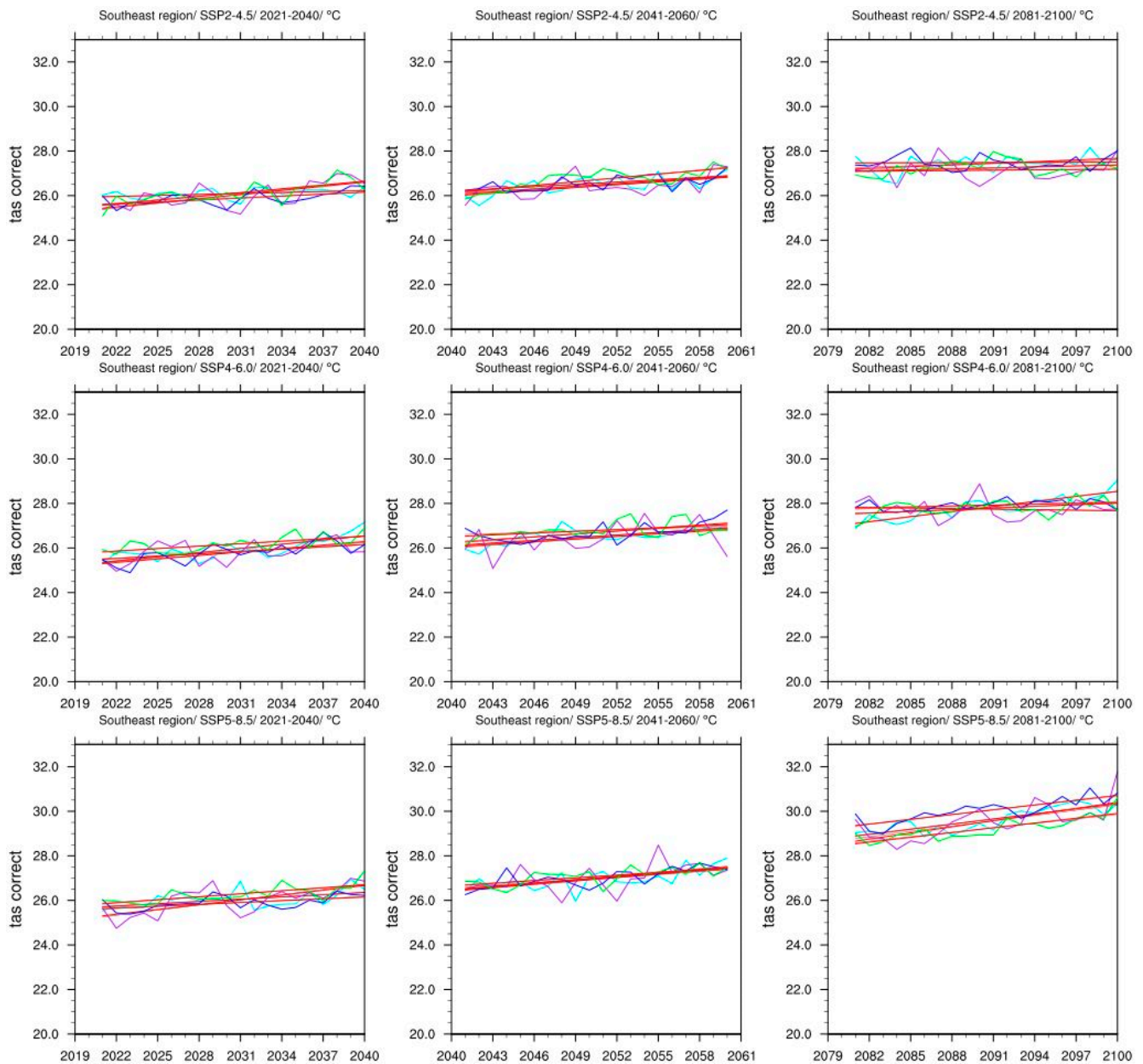


Figure 4. The same as in Figure 3 but for the southeast region.

4. Discussion

To discriminate among the three scenarios for each region, we used the *z-eq*, as recommended by [15], and the results are shown in Table 2 for the near future (for the other future periods, see Table S3). Here, we can say that the models that showed the greatest agreement with this scenario were MIROC6 and MRI-ESM2-0. For the southeast region, the SSP4-6.0 scenario was also observed to be the one with higher correspondence than SSP2-4.5 and SSP5-8.5. The models that showed agreement with SS4-6.0 were the four models for at least one of the future time periods. However, for SSP2-4.5, there were three models (CNRM-ESM2-1, IPSL-CM6A-LR, and MIROC6) in at least one of the time periods. For SSP5-8.5, they were MIROC6 and MRI-ESM2-0. For the southeast region, the SSP4-6.0 scenario was in correspondence with [15], whose scenario with radiative forcing of 6.0 W/m^2 was identified as the one that showed the same trend for the temperature variable in the

periods 2015–2039 and 2075–2099 in the observations. Remember that SSP4-6.0 is associated with SSP4 and RCP6.0 [52]. This is valid both for ERA5 and for the historical period of the models.

Table 2. Values of $z\text{-eq}$ for the four models regarding the historical period (1980–2014) of ERA5 and the models in each region (south and southeast).

Model	Scenario	Period	$z\text{-eq}$ ERA5 (South)	$z\text{-eq}$ ERA5 (Southeast)	$z\text{-eq}$ Models (South)	$z\text{-eq}$ Models (Southeast)
CNRM-ESM2-1	SSP2-4.5	2021–2040	0.68	−2.03	−1.02	−1.05
CNRM-ESM2-1	SSP4-6.0	2021–2040	2.79	1.66	1.32	2.01
CNRM-ESM2-1	SSP5-8.5	2021–2040	1.92	−0.62	0.55	−0.13
IPSL-CM6A-LR	SSP2-4.5	2021–2040	1.67	−0.93	0.36	2.15
IPSL-CM6A-LR	SSP4-6.0	2021–2040	2.60	0.87	1.61	1.08
IPSL-CM6A-LR	SSP5-8.5	2021–2040	1.67	−0.84	0.36	1.25
MIROC6	SSP2-4.5	2021–2040	1.52	1.72	0.41	2.07
MIROC6	SSP4-6.0	2021–2040	1.09	−0.51	−0.11	−0.10
MIROC6	SSP5-8.5	2021–2040	2.17	2.11	0.98	2.37
MRI_ESM2_0	SSP2-4.5	2021–2040	1.80	0.73	1.35	2.28
MRI_ESM2_0	SSP4-6.0	2021–2040	1.15	0.08	0.71	1.79
MRI_ESM2_0	SSP5-8.5	2021–2040	4.45	0.08	3.80	1.79

The z values regarding the historical data of the models for the southern region were mostly for the SSP2-4.5 scenario (with the four models for at least one of the future time periods), and for the southeast, they were mostly with SSP4-6.0 (with MIROC6 and MRI-ESM2-0). We note that the SSP4-6.0 scenario under the MIROC6 model held for the significant $z\text{-eq}$ results. Although the results were favorable for determining the scenario that maintained a trend equal to the historical one, it is not guaranteed that these trends will continue in the future.

The results of $z\text{-eq}$ assumed that the trends found under the three scenarios for the three future periods would maintain similar socio-environmental conditions to the historical ones. Therefore, we determined that the SSP4-6.0 scenario was for the southeast, which maintained these conditions under the four different models, indicating that they assumed policies with social inequality, that there are low mitigation challenges but strong challenges to adaptation. It is a scenario that has a growing population, but, by the end of the century, it will stabilize. It is also a scenario that does not demand a large amount of energy, and this is changed to the use of renewable energy [59]. The southeast of Mexico is an area highly rich in biodiversity and water resources [27], and natural resources [60], which may allow actions towards the use of clean energy. However, it has communities that are highly vulnerable to the effects of climate change [61], which is also aligned with SSP4, which indicates high social inequality and high challenges in adaptation. These results allowed us to project their impacts. The analysis of the climate indicators related to temperature and precipitation allows us to prepare for the projected impacts under the scenarios generated by the CMIP6.

In addition, the results of $z\text{-eq}$ allowed us to say that the slopes for the projected futures in the southern region are greater than the historical ones (ERA5). However, for the southeast region, the future slopes are mostly lower compared with the historical data (ERA5 and the models). This means that the scenarios projected greater warming for the southern region than for the southeast region. It should be noted that the southern zone is less hot and less humid than the southeast region [22,47,62], so this may explain this climatic result. Although the south-southeast area of Mexico is an area that has been

little studied, these results allow updates of climate information and the climate change scenarios for actions against this global phenomenon.

We can note that the warming projected for the period 2021–2040 by the scenarios had a much higher rate than the historical period. This suggests that the forcing of warming for the future period may overestimate the warming in the area. However, there was a greater correspondence with the rate of warming for the future period of 2041–2060 projected by all four models, particularly SSP4-6.0. This was attributed to the slowdown of warming by mitigation actions, following SSP4 [59]. For the same period, the other plausible scenario is SSP2-4.5, given its sustainable characteristics. Although SSP5-8.5 was also indicated by the two models, we discarded it because its non-environmentally friendly characteristics were not consistent for that period.

For the values of z between -1.96 and 1.96 , a greater number of correspondences were obtained between the slopes of the period of future projections and of the historical period. For the southern region, the scenario in which this behavior was shown by the largest number of models was SSP2-4.5. We found that for 2021–2040, the models for which the slope fell within the range of significance were CNRM-ESM2-1, IPSL-CM6A-LR, and MIROC6, while for 2041–2060, they were IPSL-CM6A-LR, MIROC6, and MRI-ESM2-0. For 2081–2100, this occurred for all four models (see Table S3). Under SSP4-6.0 for 2021–2040 and 2041–2060, it was found for only MRI-ESM2-0, and for 2081–2100, it was found for IPSL-CM6A-LR, MIROC6, and MRI-ESM2-0. Under SSP5-8.5, it was only observed for IPSL-CM6A-LR in 2021–2040, for MRI-ESM2-0 in 2041–2060, and for no model in 2081–2100. We noted that the region was assumed have of low technological development and low energy demand, given that most of its population migrates another countries to have better job options. Although the conditions may seem friendly to the environment, the region is highly vulnerable to the effects of climate change. It may involve actions that are low in mitigation and high in adaptation. That is why the SSP4.60 scenario is more likely than the SSP2-4.5 for the region.

For the southeast region, the two scenarios that had similar behavior were SSP2-4.5 and SSP4-6.0, and that are the ones that showed similar trends were three models for the period 2021–2040, four models for 2041–2060, and two models for 2081–2100. For the first scenario, the models were IPSL-CM6A-LR, MIROC6, and MRI-ESM2-0 for the first future time period, and for the last future time period, they were CNRM-ESM2-1 and MRI-ESM2-0, while for SSP4-6.0, the three scenarios in the first future time period were CNRM-ESM2-1, IPSL-CM6A-LR, and MRI-ESM2-0, and those for the last period were MRI-ESM2-0 and MIROC6. For SSP5-8.5, the models were the same as SSP2-4.5 in 2021–2040 and 2041–2060, while for 2081–2100, it was only the same as MIROC6 (see Table S3). We can say the same as we did for the southern region, namely that the scenario that can represent both the environmental and social and economic conditions of the region is SSP4-6.0.

In summary, SSP4-6.0 is a scenario with the following characteristics: it follows a medium radiative forcing and is the update of the RCP6.0 scenario. It is associated with the SSP4 family for investigating differences in the impacts across the medium global forcing scenario, even if regional climate change, land-use change, or aerosols are carried out intensively [52].

This study showed that the SSP4-6.0 scenario has characteristics that are similar to the study area. That is, the current social and economic development of the study area will allow the warming rate to remain similar to the current rate until 2040 under the current socio-environmental conditions. However, after 2024, a similar exercise to this study should be carried out, since the infrastructure of the Tren Maya [23] will drastically change the socio-environmental conditions. This is because this infrastructure has a regional impact, similar to the Interoceanic Corridor [63].

5. Conclusions

In conclusion, the downscaling technique, as suggested by [20], proved to be optimal for the temperature data, and it has yielded favorable results in the south-southeast region

of Mexico, as demonstrated in this study. By conducting a local analysis using CMIP6 scenarios, we have updated the available information for both regions. Our findings align with those of previous studies [18,53], confirming the suitability of the SSP4-6.0 scenario for the southeast region, as well as the south, when considering the significant z - eq values. However, when considering values of $-1.96 < z < 1.96$, the results indicated that SSP2-4.5 and SSP4-6.0 would be more viable options, with SSP5-8.6 being less favorable. Considering the socio-environmental characteristics of the study area, SSP4-6.0 appears to be the most realistic scenario. These results contribute to the knowledge on climate change in the region and can support local decision-making, guiding efforts towards effective adaptation and mitigation measures. Further analyses of other climatic variables and CMIP6 scenarios remain to be conducted.

Supplementary Materials: The following supporting information can be downloaded at <https://www.mdpi.com/article/10.3390/cli11050111/s1>. Figure S1: Spatial distribution of mean surface temperature (tas) with ERA5 (first column) for the south-southeast zone and the four models (CNRM-ESM2-1, IPSL-CM6A-LR, MIROC6, and MRI-ESM2-0) in the historical period 1980–2014 without (second column) and with correction (fourth column), and the bias of each one (third column). Table S1: Trend of the slopes throughout the three future periods (2021–2040, 2041–2060, and 2081–2100) with the four models (CNRM-ESM2-1, IPSL-CM6A-LR, MIROC6, and MRI-ESM2-0) and under the three scenarios SSP2-4.5, SSP4-6.0, and SSP5-8.5 with the simple difference bias correction method. Table S2: Historical trends (1980–2014) for ERA5 and the four models with bias correction. Table S3: Values of the z - eq for the four models regarding the historical period (1980–2014) and future time of the models in each region (south and southeast).

Author Contributions: Conceptualization, M.A.-V. and M.J.M.-M.; methodology, M.A.-V.; validation, M.A.-V.; formal analysis, M.A.-V.; investigation, M.A.-V. and M.J.M.-M.; data curation, M.A.-V. and M.J.M.-M.; writing—original draft preparation, M.A.-V. and M.J.M.-M.; writing—review and editing, M.A.-V. and M.J.M.-M.; visualization, M.A.-V. and M.J.M.-M.; supervision, M.A.-V. and M.J.M.-M.; project administration, M.A.-V. and M.J.M.-M.; funding acquisition, M.A.-V. All authors have read and agreed to the published version of the manuscript.

Funding: Cátedra-CONACYT under number 945 (M.A.-V.).

Data Availability Statement: We downloaded ERA5 hourly data on individual levels from 1940 and the CMIP6 climate projections to present the data from the Climate Data Store to calculate some results presented in this article. We did not download the data to redistribute it. We downloaded data from the Climate Data Store on March 2022.

Acknowledgments: We are grateful to the Cátedra-CONACYT program, particularly Project 945 (M.A.-V.). We also acknowledge CORDEX's flagship pilot study project, "North America: Dynamic Downscaling Experiments and Hydrological Modeling for Canada and Mexico", its PI José Antonio Salinas-Prieto, and María Eugenia Maya-Magaña for sharing insights on how to recover the ERA5 and CORDEX data. We acknowledge the World Climate Research Programme, which, through its Working Group on Coupled Modelling, coordinated and promoted the CMIP6. We thank the climate modeling groups for producing and making their model output available, the Earth System Grid Federation (ESGF) for archiving the data and providing access, and the multiple funding agencies who support CMIP6 and ESGF. Finally, we thank the network of researchers known as REDESClim, to which we belong.

Conflicts of Interest: The authors declare no conflict of interest. The funders had no role in the design of the study; in the collection, analyses, or interpretation of data; in the writing of the manuscript; or in the decision to publish the results.

References

1. Meehl, G.A.; Zwiers, F.; Evans, J.; Knutson, T.; Mearns, L.; Whetton, P. Trends in extreme weather and climate events: Issues related to modeling extremes in projections of future climate change. *B. Am. Meteorol. Soc.* **2000**, *81*, 427–436. [[CrossRef](#)]
2. IPCC. *Climate Change 2001: The Scientific Basis. Contribution of Working Group I to the Third Assessment Report of the Intergovernmental Panel on Climate Change*; Cambridge University Press: Cambridge, UK; New York, NY, USA, 2001; 881p.
3. IPCC. *Climate Change 2013: The Physical Science Basis. Contribution of Working Group I to the Fifth Assessment Report of the Intergovernmental Panel on Climate Change*; Cambridge University Press: Cambridge, UK; New York, NY, USA, 2013; 1535p.

4. Eyring, V.; Bony, S.; Meehl, G.A.; Senior, C.A.; Stevens, B.; Stouffer, R.J.; Taylor, K.E. Overview of the Coupled Model Intercomparison Project Phase 6 (CMIP6) experimental design and organization. *Geosci. Model Dev.* **2016**, *9*, 1937–1958. [[CrossRef](#)]
5. IPCC. Summary for Policymakers. In *Climate Change 2021: The Physical Science Basis. Contribution of Working Group I to the Sixth Assessment Report of the Intergovernmental Panel on Climate Change*; Masson-Delmotte, V., Zhai, P., Pirani, A., Connors, S.L., Péan, C., Berger, S., Caud, N., Chen, Y., Goldfarb, L., Gomis, M.I., et al., Eds.; Cambridge University Press: Cambridge, UK, 2021.
6. DKRZ. The SSP Scenarios. Deutsches Klimarechenzentrum. 2023. Available online: <https://www.dkrz.de/en/communication/climate-simulations/cmip6-en/the-ssp-scenarios> (accessed on 15 March 2023).
7. Fan, X.; Duan, Q.; Shen, C.; Wu, Y.; Xing, C. Global surface air temperatures in CMIP6: Historical performance and future changes. *Environ. Res. Lett.* **2020**, *15*, 104056. [[CrossRef](#)]
8. Almazroui, M.; Saeed, F.; Saeed, S.; Nazrul Islam, M.; Ismail, M.; Klutse, N.A.B.; Siddiqui, M.H. Projected change in temperature and precipitation over Africa from CMIP6. *Earth Syst. Environ.* **2020**, *4*, 455–475. [[CrossRef](#)]
9. Grose, M.R.; Narsey, S.; Delage, F.P.; Dowdy, A.J.; Bador, M.; Boschat, G.; Chung, C.; Kajtar, J.B.; Rauniyar, S.; Freund, M.B.; et al. Insights from CMIP6 for Australia’s future climate. *Earth’s Future* **2019**, *8*, e2019EF001469. [[CrossRef](#)]
10. You, Q.; Cai, Z.; Wu, F.; Jiang, Z.; Pepin, N.; Shen, S.S. Temperature dataset of CMIP6 models over China: Evaluation, trend and uncertainty. *Clim. Dynam.* **2021**, *57*, 17–35. [[CrossRef](#)]
11. Montero-Martínez, M.J.; Ojeda-Bustamante, W.; Santana-Sepúlveda, J.S.; Prieto-González, R.; Lobato-Sánchez, R. Sistema de consulta de proyecciones regionalizadas de cambio climático para México. *Tecnología y Ciencias del Agua* **2013**, *4*, 113–128. Available online: <https://www.scielo.org.mx/pdf/tca/v4n2/v4n2a7.pdf> (accessed on 15 March 2023).
12. Cavazos, T.; Salinas, J.A.; Martínez, B.; Colorado, G.; De Grau, P.; Prieto, R.; Conde, C.; Quintanar, A.; Santana, J.S.; Romero-Centeno, R.; et al. *Actualización de Escenarios de Cambio Climático para México como Parte de los Productos de la Quinta Comunicación Nacional; Informe Final del Proyecto al INECC: Ciudad de México, México, 2013; 150p.* Available online: <https://www.researchgate.net/publication/321274898> (accessed on 15 March 2023).
13. Fernández-Eguiarte, A.; Zavala-Hidalgo, J.; Romero-Centeno, R.; Conde-Álvarez, A.C.; Trejo-Vázquez, R.I. Actualización de los escenarios de cambio climático para estudios de impactos, vulnerabilidad y adaptación. Centro de Ciencias de la Atmósfera, Universidad Nacional Autónoma de México. Instituto Nacional de Ecología y Cambio Climático, Secretaría de Medio Ambiente y Recursos Naturales. 2015. Available online: <https://atlasclimatico.unam.mx/cmip5/visualizador> (accessed on 15 March 2023).
14. Giorgi, F.; Mearns, L.O. Calculation of Average, Uncertainty Range, and Reliability of Regional Climate Changes from AOGCM Simulations via the “Reliability Ensemble Averaging” (REA) Method. *J. Clim.* **2002**, *15*, 1141–1158. [[CrossRef](#)]
15. Andrade-Velázquez, M.; Medrano-Pérez, O.R.; Montero-Martínez, M.J.; Alcuía-Aguilar, A. Regional Climate Change in Southeast Mexico-Yucatan Peninsula, Central America and the Caribbean. *Appl. Sci.* **2021**, *11*, 8284. [[CrossRef](#)]
16. Gupta, R.; Bhattarai, R.; Mishra, A. Development of Climate Data Bias Corrector (CDBC) Tool and Its Application over the Agro-Ecological Zones of India. *Water* **2019**, *11*, 1102. [[CrossRef](#)]
17. Soriano, E.; Mediero, L.; Garijo, C. Selection of Bias Correction Methods to Assess the Impact of Climate Change on Flood Frequency Curves. *Water* **2019**, *11*, 2266. [[CrossRef](#)]
18. Iturbide, M.; Casanueva, A.; Bedia, J.; Herrera, S.; Milovac, J.; Gutiérrez, J.M. On the need of bias adjustment for more plausible climate change projections of extreme heat. *Atmos. Sci. Lett.* **2022**, *23*, e1072. [[CrossRef](#)]
19. NASA. Regional Climate Model Evaluation System. Jet Propulsion Laboratory. 2021. Available online: <https://rcmes.jpl.nasa.gov/content/statistical-downscaling> (accessed on 15 March 2023).
20. Gutiérrez, J.M.; San-Martín, D.; Brands, S.; Manzanar, R.; Herrera, S. Reassessing statistical downscaling techniques for their robust application under climate change conditions. *J. Clim.* **2013**, *26*, 171–188. [[CrossRef](#)]
21. IPCC. *Climate Change 2021: The Physical Science Basis. Contribution of Working Group I to the Sixth Assessment Report of the Intergovernmental Panel on Climate Change*; Cambridge University Press: Cambridge, UK; New York, NY, USA, 2021.
22. Andrade-Velázquez, M.; Medrano-Pérez, O.R. Historical precipitation patterns in the South-Southeast region of Mexico and future projections. *Earth Sci. Res. J.* **2021**, *25*, 69–84. [[CrossRef](#)]
23. Tren Maya. Secretaría de Turismo y Fonatur. Gobierno de México. 2023. Available online: <https://www.gob.mx/trenmaya> (accessed on 15 March 2023).
24. DTM. Seguimiento de Flujos de Población Migrante, Tenosique. Displacement Tracking Matrix. Organización Internacional para las Migraciones. ONU. 2022. Available online: <https://displacement.iom.int/sites/g/files/tmzbd11461/files/reports/DTM-Tenosique.pdf> (accessed on 15 March 2023).
25. Andrade-Velázquez, M. Visión climática de la precipitación en la cuenca del Río Usumacinta. In *La Cuenca del Río Usumacinta desde la Perspectiva del Cambio Climático*; Soares, D., García, G.A., Eds.; Instituto Mexicano de Tecnología del Agua: Jiutepec, México, 2017; pp. 1–417.
26. Andrade-Velázquez, M.; Medrano-Pérez, O.R. Precipitation patterns in Usumacinta and Grijalva basins (southern Mexico) under a changing climate. *Rev. Bio Cienc.* **2020**, *7*, 1–22. [[CrossRef](#)]
27. UNEP. Climate Action, What We Do, Climate Adaptation. United Nations Environment Programme. 2023. Available online: <https://www.unep.org/explore-topics/climate-action/what-we-do/climate-adaptation/ecosystem-based-adaptation> (accessed on 15 March 2023).

28. Hersbach, H.; Bell, B.; Berrisford, P.; Biavati, G.; Horányi, A.; Muñoz Sabater, J.; Nicolas, J.; Peubey, C.; Radu, R.; Rozum, I.; et al. ERA5 Hourly Data on Pressure Levels from 1940 to Present. Copernicus Climate Change Service (C3S) Climate Data Store (CDS). 2023. Available online: <https://doi.org/10.24381/cds.bd0915c6> (accessed on 15 March 2023).
29. Salinas, J.A.; Maya, M.E.; Hernández, C.; Montero-Martínez, M.J. *Informe Final del Proyecto de Investigación Interno "Evaluación de Modelos Atmosféricos Globales del Experimento CMIP6 para México. Cuantificación de Impactos de Eventos Extremos y Cambio Climático"*; Instituto Mexicano de Tecnología del Agua: Jiutepec, México, 2020.
30. Rivera, P. Evaluation of Historical Simulations of CMIP6 Models for Temperature and Precipitation in Guatemala. *Earth Syst. Environ.* **2023**, *7*, 43–65. [[CrossRef](#)]
31. Seferian, R. CNRM-CERFACS CNRM-ESM2-1 Model Output Prepared for CMIP6 CMIP Historical. Earth System Grid Federation. 2018. Available online: <https://www.wdc-climate.de/ui/cmip6?input=CMIP6.CMIP.CNRM-CERFACS.CNRM-ESM2-1.historical> (accessed on 15 March 2023).
32. Voldoire, A. CNRM-CERFACS CNRM-ESM2-1 Model Output Prepared for CMIP6 ScenarioMIP SSP245. Earth System Grid Federation. 2019. Available online: <https://www.wdc-climate.de/ui/cmip6?input=CMIP6.ScenarioMIP.CNRM-CERFACS.CNRM-ESM2-1.ssp245> (accessed on 15 March 2023).
33. Voldoire, A. CNRM-CERFACS CNRM-ESM2-1 Model Output Prepared for CMIP6 ScenarioMIP SSP460. Earth System Grid Federation. 2019. Available online: <https://www.wdc-climate.de/ui/cmip6?input=CMIP6.ScenarioMIP.CNRM-CERFACS.CNRM-ESM2-1.ssp460> (accessed on 15 March 2023).
34. VOLDOIRE, A. CNRM-CERFACS CNRM-ESM2-1 MODEL output prepared for CMIP6 ScenarioMIP SSP585. Earth System Grid Federation. 2019. Available online: <https://www.wdc-climate.de/ui/cmip6?input=CMIP6.ScenarioMIP.CNRM-CERFACS.CNRM-ESM2-1.ssp585> (accessed on 15 March 2023).
35. Boucher, O.; Denvil, S.; Levassasseur, G.; Cozic, A.; Caubel, A.; Foujols, M.-A.; Meurdesoif, Y.; Cadule, P.; Devilliers, M.; Ghattas, J.; et al. IPSL IPSL-CM6A-LR Model Output Prepared for CMIP6 CMIP Historical. Earth System Grid Federation. 2018. Available online: <https://www.wdc-climate.de/ui/cmip6?input=CMIP6.CMIP.IPSL.IPSL-CM6A-LR.historical> (accessed on 15 March 2023).
36. Boucher, O.; Denvil, S.; Levassasseur, G.; Cozic, A.; Caubel, A.; Foujols, M.-A.; Meurdesoif, Y.; Cadule, P.; Devilliers, M.; Dupont, E.; et al. IPSL IPSL-CM6A-LR Model Output Prepared for CMIP6 ScenarioMIP SSP245. Earth System Grid Federation. 2019. Available online: <https://www.wdc-climate.de/ui/cmip6?input=CMIP6.ScenarioMIP.IPSL.IPSL-CM6A-LR.ssp245> (accessed on 15 March 2023).
37. Boucher, O.; Denvil, S.; Levassasseur, G.; Cozic, A.; Caubel, A.; Foujols, M.-A.; Meurdesoif, Y.; Cadule, P.; Devilliers, M.; Dupont, E.; et al. IPSL IPSL-CM6A-LR Model Output Prepared for CMIP6 ScenarioMIP SSP460. Earth System Grid Federation. 2019. Available online: <https://www.wdc-climate.de/ui/cmip6?input=CMIP6.ScenarioMIP.IPSL.IPSL-CM6A-LR.ssp460> (accessed on 15 March 2023).
38. Boucher, O.; Denvil, S.; Levassasseur, G.; Cozic, A.; Caubel, A.; Foujols, M.-A.; Meurdesoif, Y.; Cadule, P.; Devilliers, M.; Dupont, E.; et al. IPSL IPSL-CM6A-LR Model Output Prepared for CMIP6 ScenarioMIP SSP585. Earth System Grid Federation. 2019. Available online: <https://www.wdc-climate.de/ui/cmip6?input=CMIP6.ScenarioMIP.IPSL.IPSL-CM6A-LR.ssp585> (accessed on 15 March 2023).
39. Tatebe, H.; Watanabe, M. MIROC MIROC6 Model Output Prepared for CMIP6 CMIP Historical. Earth System Grid Federation. 2018. Available online: <https://www.wdc-climate.de/ui/cmip6?input=CMIP6.CMIP.MIROC.MIROC6.historical> (accessed on 15 March 2023).
40. Shiogama, H.; Abe, M.; Tatebe, H. MIROC MIROC6 Model Output Prepared for CMIP6 ScenarioMIP SSP245. Earth System Grid Federation. 2019. Available online: <https://www.wdc-climate.de/ui/cmip6?input=CMIP6.ScenarioMIP.MIROC.MIROC6.ssp245> (accessed on 15 March 2023).
41. Shiogama, H.; Abe, M.; Tatebe, H. MIROC MIROC6 Model Output Prepared for CMIP6 ScenarioMIP SSP460. Earth System Grid Federation. 2019. Available online: <https://www.wdc-climate.de/ui/cmip6?input=CMIP6.ScenarioMIP.MIROC.MIROC6.ssp460> (accessed on 15 March 2023).
42. Shiogama, H.; Abe, M.; Tatebe, H. MIROC MIROC6 Model Output Prepared for CMIP6 ScenarioMIP SSP585. Earth System Grid Federation. 2019. Available online: <https://www.wdc-climate.de/ui/cmip6?input=CMIP6.ScenarioMIP.MIROC.MIROC6.ssp585> (accessed on 15 March 2023).
43. Yukimoto, S.; Koshiro, T.; Kawai, H.; Oshima, N.; Yoshida, K.; Urakawa, S.; Tsujino, H.; Deushi, M.; Tanaka, T.; Hosaka, M.; et al. MRI MRI-ESM2.0 Model Output Prepared for CMIP6 CMIP Historical. Earth System Grid Federation. 2019. Available online: <https://www.wdc-climate.de/ui/cmip6?input=CMIP6.CMIP.MRI.MRI-ESM2-0.historical> (accessed on 15 March 2023).
44. Yukimoto, S.; Koshiro, T.; Kawai, H.; Oshima, N.; Yoshida, K.; Urakawa, S.; Tsujino, H.; Deushi, M.; Tanaka, T.; Hosaka, M.; et al. MRI MRI-ESM2.0 Model Output Prepared for CMIP6 ScenarioMIP SSP245. Earth System Grid Federation. 2019. Available online: <https://www.wdc-climate.de/ui/cmip6?input=CMIP6.ScenarioMIP.MRI.MRI-ESM2-0.ssp245> (accessed on 15 March 2023).
45. Yukimoto, S.; Koshiro, T.; Kawai, H.; Oshima, N.; Yoshida, K.; Urakawa, S.; Tsujino, H.; Deushi, M.; Tanaka, T.; Hosaka, M.; et al. MRI MRI-ESM2.0 Model Output Prepared for CMIP6 ScenarioMIP SSP460. Earth System Grid Federation. 2019. Available online: <https://www.wdc-climate.de/ui/cmip6?input=CMIP6.ScenarioMIP.MRI.MRI-ESM2-0.ssp460> (accessed on 15 March 2023).

46. Yukimoto, S.; Koshiro, T.; Kawai, H.; Oshima, N.; Yoshida, K.; Urakawa, S.; Tsujino, H.; Deushi, M.; Tanaka, T.; Hosaka, M.; et al. MRI MRI-ESM2.0 Model Output Prepared for CMIP6 ScenarioMIP SSP585. Earth System Grid Federation. 2019. Available online: <https://www.wdc-climate.de/ui/cmip6?input=CMIP6.ScenarioMIP.MRI.MRI-ESM2-0.ssp585> (accessed on 15 March 2023).
47. FIDESUR. Fideicomiso para el Desarrollo Regional del Sur Sureste. 2023. Available online: <https://sursureste.org.mx/> (accessed on 15 March 2023).
48. Kendall, M.G. *Rank Correlation Methods*; Charles Griffin: London, UK, 1948.
49. Lehmann, E.L.; D'Abbrera, H.J. *Nonparametrics Statistical Methods Based on Ranks*; Holden-Day: San Francisco, CA, USA, 1975.
50. Clogg, C.C.; Petkova, E.; Haritou, A. Statistical methods for comparing regression coefficients between models. *Am. J. Sociol.* **1995**, *100*, 1261–1293. Available online: <http://www.jstor.org/stable/2782277> (accessed on 15 March 2023). [[CrossRef](#)]
51. Paternoster, R.; Brame, R.; Mazerolle, P.; Piquero, A. Using the correct statistical test for the equality of regression coefficients. *Criminology* **1998**, *36*, 859–866. [[CrossRef](#)]
52. O'Neill, B.C.; Tebaldi, C.; van Vuuren, D.P.; Eyring, V.; Friedlingstein, P.; Hurtt, G.; Knutti, R.; Kriegler, E.; Lamarque, J.-F.; Lowe, J.; et al. The Scenario Model Intercomparison Project (ScenarioMIP) for CMIP6. *Geosci. Model Dev.* **2016**, *9*, 3461–3482. [[CrossRef](#)]
53. Almazroui, M.; Islam, M.N.; Saeed, F.; Saeed, S.; Ismail, M.; Ehsan, M.A.; Diallo, I.; O'Brien, E.; Ashfaq, M.; Martínez-Castro, D.; et al. Projected Changes in Temperature and Precipitation Over the United States, Central America, and the Caribbean in CMIP6 GCMs. *Earth Syst. Environ.* **2021**, *5*, 1–24. [[CrossRef](#)]
54. Harris, I.; Jones, P.D.; Osborn, T.J.; Lister, D.H. Updated high-resolution grids of monthly climatic observations—The CRU TS3.10 Dataset. *Int. J. Climat.* **2014**, *34*, 623–642. [[CrossRef](#)]
55. Peralta-Hernandez, A.R.; Balling, R.C., Jr.; Barba-Martinez, L.R. Analysis of near-surface diurnal temperature variations and trends in southern Mexico. *Int. J. Clim.* **2009**, *29*, 205–209. [[CrossRef](#)]
56. Cavazos, T.; Luna-Niño, R.; Cerezo-Mota, R.; Fuentes-Franco, R.; Méndez, M.; Pineda Martínez, L.F.; Valenzuela, E. Climatic trends and regional climate models intercomparison over the CORDEX-CAM (Central America, Caribbean, and Mexico) domain. *Int. J. Clim.* **2020**, *40*, 1396–1420. [[CrossRef](#)]
57. Murray-Tortarolo, G.N. Seven decades of climate change across Mexico. *Atmósfera* **2021**, *34*, 217–226. [[CrossRef](#)]
58. INEGI. Cuentame, Información por Entidad. Instituto Nacional de Estadística y Geografía. 2023. Available online: <https://cuentame.inegi.org.mx/monografias/default.aspx?tema=me> (accessed on 15 March 2023).
59. Riahi, K.; Van Vuuren, D.P.; Kriegler, E.; Edmonds, J.; O'Neill, B.C.; Fujimori, S.; Bauer, N.; Calvin, K.; Dellink, R.; Fricko, O. The Shared Socioeconomic Pathways and their energy, land use, and greenhouse gas emissions implications: An overview. *Global Environ. Change* **2017**, *42*, 153–168. [[CrossRef](#)]
60. Monroy-Martínez, J.M. *Plan Puebla-Panamá como Estrategia ante la Problemática de Atraso en el Sur-Sureste Mexicano. Tesis. Relaciones Internacionales*; Escuela de Ciencias Sociales, Universidad de las Américas Puebla: Cholula, México, 2003; Available online: http://catarina.udlap.mx/u_dl_a/tales/documentos/lri/monroy_m_jm/ (accessed on 15 March 2023).
61. García, A.G.; Kauffer, E.F.M. Las cuencas compartidas entre México, Guatemala y Belice: Un acercamiento a su delimitación y problemática general. *Front. Norte* **2011**, *23*, 131–161. Available online: <http://www.redalyc.org/articulo.oa?id=13618448005>> (accessed on 15 March 2023).
62. INEGI. Climatología. Geografía y Medioambiente. Mapas. Instituto Nacional de Estadística y Geografía. 2023. Available online: <https://www.inegi.org.mx/temas/climatologia/> (accessed on 15 March 2023).
63. Corredor Interoceánico. Gobierno de México. 2023. Available online: <https://www.gob.mx/ciit> (accessed on 15 March 2023).

Disclaimer/Publisher's Note: The statements, opinions and data contained in all publications are solely those of the individual author(s) and contributor(s) and not of MDPI and/or the editor(s). MDPI and/or the editor(s) disclaim responsibility for any injury to people or property resulting from any ideas, methods, instructions or products referred to in the content.